Drug Design, Development and Therapy

Dovepress

open access to scientific and medical research

Open Access Full Text Article

ORIGINAL RESEARCH

MsrA Suppresses Inflammatory Activation of Microglia and Oxidative Stress to Prevent Demyelination via Inhibition of the NOX2-MAPKs /NF-κB Signaling Pathway

This article was published in the following Dove Press journal:
Drug Design, Development and Therapy

Hua Fan[1,*]
Damiao Li[1,*]
Xinlei Guan[2,*]
Yanhui Yang[1]
Junqiang Yan[1]
Jian Shi[1]
Ranran Ma[3]
Qing Shu[3]

[1]The First Affiliated Hospital, College of Clinical Medicine of Henan University of Science and Technology, Luoyang 471000, People's Republic of China; [2]Department of Pharmacy, Wuhan Puai Hospital, Tongji Medical College, Huazhong University of Science and Technology, Wuhan 430030, People's Republic of China; [3]Department of Pharmacy, Ninth Hospital of Xi'an, Affiliated to Medical College of Xi'an Jiaotong University, Xi'an 710054, People's Republic of China

*These authors contributed equally to this work

Correspondence: Hua Fan
The First Affiliated Hospital, College of Clinical Medicine of Henan University of Science and Technology, No. 24, Jinghua Road, Jianxi District, Luoyang 471000, Henan Province, People's Republic of China
Tel +86-18538825892
Email fanhua19851229@126.com

Qing Shu
Department of Pharmacy, Ninth Hospital of Xi'an, Affiliated to Medical College of Xi'an Jiaotong University, No. 151, Eastern Section of South 2nd Ring Road, Xi'an 710054, Shaanxi Province, People's Republic of China
Tel +86-18627121873
Email shuqinglwz@163.com

Introduction: Demyelination causes neurological deficits involving visual, motor, sensory symptoms. Deregulation of several enzymes has been identified in demyelination, which holds potential for the development of treatment strategies for demyelination. However, the specific effect of methionine sulfoxide reductase A (MsrA) on demyelination remains unclear. Hence, this study aims to explore the effect of MsrA on oxidative stress and inflammatory response of microglia in demyelination.

Methods: Initially, we established a mouse model with demyelination induced by cuprizone and a cell model provoked by lipopolysaccharide (LPS). The expression of MsrA in wild-type (WT) and MsrA-knockout ($MsrA^{-/-}$) mice were determined by RT-qPCR and Western blot analysis. In order to further explore the function of MsrA on inflammatory response, and oxidative stress in demyelination, we detected the expression of microglia marker Iba1, inflammatory factors TNF-α and IL-1β and intracellular reactive oxygen species (ROS), superoxide dismutase (SOD) activity, as well as expression of the NOX2-MAPKs/NF-κB signaling pathway-related genes in $MsrA^{-/-}$ mice and LPS-induced microglia following different treatments.

Results: MsrA expression was downregulated in $MsrA^{-/-}$ mice. MsrA silencing was shown to produce severely injured motor coordination, increased expressions of Iba1, TNF-α, IL-1β, ROS and NOX2, and extent of ERK, p38, IκBα, and p65 phosphorylation, but reduced SOD activity. Conjointly, our study suggests that Tat-MsrA fusion protein can prevent the cellular inflammatory response and subsequent demyelination through negative regulation of the NOX2-MAPKs/NF-κB signaling pathway.

Conclusion: Our data provide a profound insight on the role of endogenous antioxidative defense systems such as MsrA in controlling microglial function.

Keywords: demyelination, MsrA, NOX2-MAPKs/NF-κB signaling pathway, microglia, oxidative stress, inflammatory activation

Introduction

Demyelination refers to a loss of myelin with associated preservation of axons which plays a critical role in the transmission of neural signal in the central nervous system.[1] The types of demyelinating disease include multiple sclerosis (MS), progressive multifocal leukoencephalopathy, acute-disseminated encephalomyelitis, and extrapontine myelinolysis.[1] Demyelination is a critical pathologic hallmark in MS, which is a complicated neurological disease affecting millions of people

worldwide.[2] The most prevalent manifestation of MS patients is compensated mobilization, due to which almost half of patients become dependent on walking aids and need a wheelchair for more than a decade with the disease.[3] Glial cells are reported to act as neuronal supportive cells and keep the health of the neurons.[4] Besides, abnormally activated microglia can facilitate the production of multiple kinds of pro-inflammatory mediators such as cytokines, chemokines and reactive oxygen species (ROS) that are deemed to enhance the inflammatory cascade and to induce neuronal damage by activating oxidative stress and several programmed cell-death pathways.[5] It is reported that inflammatory reactions are well-known important course of the secondary damage cascade, including inflammatory cell infiltration as well as neuronal and glial cell destruction.[6] Interestingly, a previous study has suggested that an autoimmune inflammatory reaction potentially leads to demyelination and axonal damage in the central nervous system which can result in chronic inflammatory demyelinating disease.[7]

A recent study has reported that enzymes involving metabolism are related to the treatment of central nervous system diseases,[8] which emphases the need to further explore the molecular mechanisms of enzymes in demyelination. Methionine sulfoxide reductase A (MsrA), an antioxidant enzyme, exerts a critical function in cell and tissue protection, and its interaction with other proteins or growth factors holds potential to provide a target for therapeutic modalities to combat degenerative diseases.[9] An existing study has reported that MsrA, as one of the antioxidant defenses in cells, is crucial in the prevention of oxidative stress-related disease.[10] Although oxidative stress has been proven to be one inducer of demyelination; however, no direct evidence supports the speculation that MsrA is related to demyelination. NADPH oxidases (NOX) enzymes function as a mediator to transfer electrons across membranes, which then react with oxygen generating the superoxide anion O^{2-}.[11] Currently five NOX family members (NOX1-5) have been identified, and NOX2 is typically classified in the brain and neurons.[12] NOX enzymes function as major producers of ROS, which regulates the progression of central nervous system disorders, and ROS and NOX2 have been reported to serve as regulators of fundamental neuronal functions and neuroinflammatory processes in the central nervous system.[11] One study flagged the ability of MsrA to use NADPH to reduce the oxidized form of methionine back to its reduced form thus serving as a barrier for protecting the proteins.[13] In another study, it is also suggested that NOX2-dependent ROS generation can result in activation of the mitogen-activated protein kinase (MAPK) and downstream transcription factors nuclear factor-κB (NF-κB).[14] In the current study, we assumed that MsrA affects demyelination by regulating the NOX2-MAPKs /NF-κB signaling pathway, and we aimed to explore the molecular mechanisms of MsrA in oxidative stress and inflammatory activation by mediating the NOX2-MAPKs /NF-κB signaling pathway in demyelination.

Materials and Methods

Ethics Statement

This study was conducted in strict accordance with the recommendations in the Guide for the Care and Use of Laboratory Animals of the National Institutes of Health. The experimental protocols were approved by the Institutional Animal Care and Use Committee of the First Affiliated Hospital, and College of Clinical Medicine of Henan University of Science and Technology. Optimal measures were taken to minimize the usage of animals as well as their suffering.

Preparation of MsrA Knockout Mice ($MsrA^{-/-}$) Mice by Small Hairpin RNA (shRNA) Lentivirus in vivo and Wild-Type (WT) Mice

Eighty normal WT C57BL/6 mice were purchased from the Beijing Vital River Laboratory Animal Technology Company (Beijing, China), among which $MsrA^{-/-}$ mice were prepared by shRNA lentivirus in 40 mice.

MsrA gene was amplified by conducting polymerase chain reaction. The shRNAs were constructed using the third generation of self-inactivated lentiviral vectors containing a CMV-driven GFP reporter and a U6 promoter upstream of the cloning sites (Age I and EcoR I) (Shanghai Genechem Co., Ltd., Shanghai, China) and sequenced.[15]

The shRNAs were injected into the corpus callosum of $MsrA^{-/-}$ mice. The anesthetized mice were then positioned in a stereotactic framework (Narishige, Tokyo, Japan). A stereotactic injection of shRNA was instilled in the corpus callosum (anteroposterior - 1.0 mm from bregma, mediolateral + 0.5 mm from the midline, dorsoventral - 1.0 mm from dura). A Hamilton syringe (31 gauge, Sigma-Aldrich Chemical Company, St Louis, MO, USA) connected to the microsyringe (IMS-3, Narishige, Tokyo, Japan) was

inserted into the corpus callosum and sustained for 3 min before injecting each sample (1 μL).[16]

Establishment of Cuprizone-Induced Demyelination Mouse Models

All mice (6-weeks old, weighing 18–22 g) were housed in a room (12 h day/night alternate cycles) under controlled temperature and humidity. Mice were fed with food powder containing 0.2% (w/w) cuprizone (Sigma-Aldrich Chemical Company, St Louis, MO, USA) for 4 weeks while the control mice were fed normal food. Food containing cuprizone was renewed every 2 days for 4 weeks.[17] The mice were then assigned into the WT (WT mice, n = 20), the $MsrA^{-/-}$ (MsrA knockout mice, n = 20), the WT + cuprizone (WT mice treated with cuprizone, n = 20) and the $MsrA^{-/-}$ + cuprizone (MsrA knockout mice treated with cuprizone, n = 20) groups.

Brain Tissue and Microglia Extraction

Mice were anesthetized using 3% sodium pentobarbital solution (P3761, Sigma-Aldrich Chemical Company, St Louis, MO, USA). The chest was excavated and flushed with saline through the heart, after which the brain tissue was isolated. The brain tissue of 10 mice from each group was stored in liquid nitrogen for reverse transcription quantitative polymerase chain reaction (RT-qPCR) and Western blot analysis, respectively. The brain tissues of remaining 10 mice in each group were dissected and one hemisphere was fixated using 4% paraformaldehyde overnight. The brain tissue was then immersed in 20% diethyl phosphorocyanidate (DEPC) sucrose water. After sedimentation, the brain tissue was extracted, and embedded with optical coherence tomography (OCT). Then the corpus callosum was isolated for preparing frozen coronal sections. The other hemisphere was used to isolate microglia, respectively.

According to the provided instructions, the tissue was homogenized using a mild MACS™ Dissociator (Miltenyi Biotec, Bisley, Surrey, UK). The separated tissues were filtered, rinsed and centrifuged. The precipitates containing the microglia were resuspended. The tissue was then stained with CD11b beads (Miltenyi Biotec, Bisley, Surrey, UK) and magnetically separated using the QuadroMACS separator (Miltenyi Biotec, Bisley, Surrey, UK) in strict accordance with the provided instructions. The sample was resuspended and the final microglia precipitate was resuspended in phosphate-buffered saline (PBS) (75 μL). The cells were seeded in multiple 48-well plates (2.5×10^4 cells/well, final volume 200 μL) and cultured using Dulbecco's modified Eagle's medium (DMEM) supplemented with a combination of M-CSF (100 ng/mL; R&D Systems, UK) and GM-CSF (100 ng/mL; R&D Systems, UK). The microglia were adapted for 5 days, and the culture medium was replaced on alternate days. On the 5th day, the relevant experiments were conducted. Lipopolysaccharide (LPS) treatment was conducted on the 9th day after culture.[18]

Rotarod Test

Coordination and balance of mice were evaluated using a rotarod instrument (Med Associates Inc, St. Albans, VT, USA). The mice were evaluated daily on a carousel, at a speed between 8 r/min and 80 r/min. The grabbing time for each mouse and an average of nine trials for 3 consecutive days (3 times a day) were recorded.[19]

Oil Red O Staining

After anesthesia, the mice were perfused with PBS and then with 4% paraformaldehyde solution. The brain underwent perfusion with different concentrations of sucrose solution (15–30%) to facilitate the formation of 15 mm frozen brain sections. Frozen sections were then incubated using distilled water for 1 min and 100% propylene glycol (Polyscientific, Bayshore, NY, USA) for 2 min. A section was transferred to Oil red O for 36 h at room temperature and the other section was incubated using 85% propylene glycol for 1 min, stained with hematoxylin and fixed using the gelatin fixation medium.

Immunofluorescence Assay

After rewarming, the sections were rinsed three times with 0.01 mol/L PBS, after which section was blocked using bovine serum albumin (BSA) in PBS solution. Then, the sections were incubated at 4°C overnight with several primary antibodies including the rabbit antibody to 2′,3′-cyclic nucleotide 3′-phosphodiesterase (CNP) (1:10,000, ab227218, Abcam Inc., Cambridge, MA, USA), rabbit antibody to Olig2 (1:100, ab42453, Abcam Inc., Cambridge, MA, USA), rabbit antibody to Iba1 (1:100, ab178847, Abcam Inc., Cambridge, MA, USA) and mouse antibody to Iba1 (1:200, ab6319, Abcam Inc., Cambridge, MA, USA). Next, the sections were supplemented with secondary antibodies including the goat anti-rabbit IgG (1:200, ab150077, Abcam Inc., Cambridge, MA, USA) and goat anti-mouse IgG (1:1000, ab150113, Abcam Inc.,

Cambridge, MA, USA). The nucleus was stained with 4′-6-diamidino-2-phenylindole (DAPI). A section was blocked using the fluorescent quenching agent and observed under a microscope with five visual fields. Photoshop CS3 software was used for cell counting.

RT-qPCR

Total RNA was extracted using Trizol (15596026, Invitrogen, Carlsbad, California, USA), which was reversely transcribed into complementary DNA (cDNA) using the RT kit (RR047A, Takara Bio Inc., Otsu, Shiga, Japan). Using the SYBR Premix EX Taq kit (RR420A, Takara Bio Inc., Otsu, Shiga, Japan), RT-qPCR was performed on an ABI 7500 instrument (Applied Biosystems, Foster City, CA, USA). Three duplicated wells were set for each sample. Primers were synthesized and provided by Shanghai Sangon Biotechnology Co., Ltd. (Shanghai, China) (Table 1). With β-actin and glyceraldehyde-3-phosphate dehydrogenase (GAPDH) serving as internal references, the fold changes were calculated based on relative quantification ($2^{-\Delta\Delta Ct}$ method).

Western Blot Analysis

The total proteins were extracted from tissues and cells using the radio-immunoprecipitation assay (RIPA) lysis buffer containing proteinase inhibitor phenylmethylsulfonyl fluoride (PMSF) and incubated on ice at 4°C for 30 min. After a regimen of centrifugation at 4°C and 8000 g for 10 min, the supernatant was collected. Total protein concentration was measured using a bicinchoninic acid protein assay kit. The protein (50 μg) was subjected to sodium dodecyl sulfate-polyacrylamide gel electrophoresis (SDS-PAGE) treatment and subsequently transferred onto polyvinylidene difluoride membranes by the wet transfer method. Membrane was blocked using 5% skim milk for 1 h at room temperature and probed at 4°C overnight with the following primary rabbit antibodies from Abcam Inc. (Cambridge, MA, USA): MsrA (1:2000, ab16803), CNP (1:10,000, ab227218), NOX2 (1:1000, ab80508), extracellular signal-regulated kinase (ERK) (1:1000, ab184699), phosphorylated ERK (p-ERK, 1:1000, ab201015), p38 (1:1000, ab225534), phosphorylated p38 (p-p38, 1:1000, ab47363), JNK (1:1000, ab179461), phosphorylated JNK (p-JNK, 1:10,000, ab124956), IκBα (1:10,000, ab32518), phosphorylated IκBα (p-IκBα, 1:10,000, ab133462), p65 (1:1000, ab16502), phosphorylated p65 (p-p65, 1:2000, ab86299), and GAPDH (1:10,000, ab181602). After a rinse, the membrane was incubated with the horseradish peroxidase-conjugated secondary antibody (1:10,000, ab6721, Abcam Inc., Cambridge, MA, USA). The immunocomplexes on the membrane were visualized using the enhanced chemiluminescence (ECL) fluorescence test kit (BB-3501, Amersham Pharmacia Biotech, Little Chalfont, United Kingdom) and band intensities were quantified using the Bio-Rad image analysis system (BIO-RAD Laboratories, CA, USA) and the Quantity One v4.6.2 software. The relative protein expression was expressed as the gray value of the corresponding protein band to that of the GAPDH protein band.

Table 1 Primer Sequences for RT-qPCR

Gene	Sequences
MsrA	F: 5′-CTGGGAGAATCACGACCCG-3′ R: 5′-CGGATGTGGGATAGACTGCT-3
β-actin	F: 5′-GCCTTCCTTCTTGGGTAT-3′ R: 5′-GGCATAGAGGTCTTTACGG-3′
GAPDH	F: 5′-TGACTTCAACAGCGACACCCA-3′ R: 5′-CACCCTGTTGCTGTAGCCAAA-3′

Abbreviations: RT-qPCR, reverse transcription quantitative polymerase chain reaction; F, forward; R, reverse; MsrA, methionine sulfoxide reductase A; GAPDH, glyceraldehyde-3-phosphate dehydrogenase.

Detection of Intracellular ROS Level

Dichlorofluorescin diacetate (DCFH-DA) and flow cytometry were conducted to detect the level of intracellular ROS. A total of 1×10^6 cells was detached using ethylenediaminetetraacetic acid-free trypsin and immersed in ice-cold PBS. Then the supernatant was discarded after centrifugation. DCFH-DA was diluted to 10 μmol/L using serum-free medium. The cells were incubated under conditions devoid of light for 10 min, and finally rinsed once with PBS. Flow cytometry was adopted for quantitative detection of the fluorescence intensity of dichlorofluorescein (DCF) after an ice bath. DCF exhibiting green fluorescence depicted the emission wavelength of 530 nm and the average fluorescence intensity value = total fluorescence intensity value/total cells.

Detection of Superoxide Dismutase (SOD) Activity

Superoxide anion (O^{2-}) was produced by xanthine and the xanthine oxidase reaction system. O^{2-} could reduce nitroblue tetrazolium to blue formazan, which was absorbed at 560 nm. SOD could remove O^{2-}, accordingly inhibiting the formation of formazan. The appearance of navy blue of the reaction solution was indicative of lower activity of SOD,

and otherwise, the activity of SOD was higher. The activity of SOD in microglia of mice was detected in a similar manner. The specific steps were conducted in strict accordance to the provided instructions of the SOD determination kit (BC0175, Beijing Solarbio Science & Technology Co., Ltd., Beijing, China). The activity of SOD was calculated in accordance to the formula enlisted in the instructions.

Enzyme-Linked Immunosorbent Assay (ELISA)

With detection of interleukin (IL)-1β for example, the mouse microglia in the logarithmic growth phase were cultured in serum-free DMEM for 24 h. Cell supernatants from each group were collected the following day, and 2 mL of supernatants were taken for vacuum freeze-drying and dissolved in 100 μL diluent. The microporous plate was sealed using 50 μL standard solution or sample solution per well, incubated for 2 h and then rinsed 5 times. Next, the plate was incubated for 30 min after supplementation with 50 μL streptavidin-peroxidase solution in each well. Subsequently, 50 μL substrate was added to the plate for incubation for 10 min after which 50 μL of terminating solution was added and the color changed from green to yellow. A microplate reader (Bio-Rad Laboratories, Hercules, CA, USA) was adopted to record the absorbance value at 450 nm. The detection of tumor necrosis factor-α (TNF-α) level was performed according to the aforementioned procedures. IL-1β (ML-Elisa-0378, R&D Systems, Minneapolis, MN, USA) and TNF-α (RAB0477, Sigma-Aldrich Chemical Company, St Louis, MO, USA) kits were used.

Tat-MsrA Protein Preparation

The cDNA fragment encoding MsrA was derived from pcDNA3.1-MsrA. The pET-32a (+) vector and amplification products were detached using BamHI and XhoI (MBI) endonucleases (MBIFERMENTAS, Burlington, ON, Canada). Then the complete PCR fragment of the mouse MsrA coding region was ligated to the restriction pET-32a (+) vector using the phage T4 ligase (MBI Fermentas, Burlington, ON, Canada). The insertion of the MsrA cDNA in pET-32a (+) vector was determined at least twice in each direction. BL21 cell transformation and recombinant plasmids were cultured in luria-bertani (LB) medium containing ampicillin (50 μg/mL) at 37°C. When the absorbance of the cells at an excitation wavelength of 600 nm was 0.7, 0.5 mM IPTG (Amresco, Cochran solon, OH, USA) was added to the medium to attain the final concentration for further incubation for 4 h. The cells after centrifugation were suspended in buffer A (20 mM Tris-HCl, 0.5 mM imidazole and 500 mM NaCl) and subjected to ultrasound treatment for 4 times, 30 s each time. Next, the supernatant was added to a 4 mL Ni-Trap nickel chelate column (Qiagen GE Healthcare, Hilden, Germany). Subsequently, the recombinant peptide containing the entire MsrA protein was eluted with buffer A, and 5 mL of protein concentrate was isolated by the centrifugation ultrafiltration method. The His tag at the N end of the recombinant peptide was removed using a thrombin kit (New England Biolabs, Ipswich, MA, USA). The protein (500 μg) was detached at 20°C for 24 h. The purity of the recombinant protein was confirmed by SDS-PAGE and Coomassie blue staining. The recombinant protein MsrA was stored at −80°C for further experiments.

Analysis of the Activity of Tat-MsrA

Tat-rMsrA activity was monitored by detection of Meto reduction activity. Firstly, 20 μg of recombinant Tat-rMsrA protein was added to the reaction mixture (pH = 7.4) containing 50 mM sodium phosphate, 10 mm $MgCl_2$, 30 mm KCl, 20 mm dithiothreitol (DTT, Sigma-Aldrich, St. Louis, MO, USA) and 0.5 mM MetO (Sigma-Aldrich, St. Louis, MO, USA). The mixture was incubated at 37°C for 30 min and the reaction was terminated by the addition of diamine. The content of Tat-rMsrA was monitored under a combination method of liquid chromatography and electrospray. After inactivation of Tat-MsrA, Meto reduction activity was not detectable. The activity of recombinant Tat-rMsrA was determined by colorimetric analysis before each experiment. Different concentrations of recombinant rMsrA peptide (active or inactive) were added to the reaction buffer to facilitate incubation. Due to the potential reduction activity of DTT, the reaction was conducted in a airtight and dark atmosphere. Then, DTT was incubated after supplementing 100 μL reaction mixture and 100 μL dithionitrobenzoate (DTNB) (4 mM) for 10 min. The absorbance at 412 nm was measured using a microplate reader (ELx800, Bio Tek, Instrument, Inc., Winooski, VT, USA). The optical density (OD) value at 0 min in the incubation was defined as the initial value, and compared with the initial value, the decrease (Δ) in OD at 412 nm after completion of the reaction was calculated and monitored.

Culture of LPS-Induced Microglia in vitro

Mouse microglia were purchased from the Basic Medical Cell Center of the Institute of Basic Medical Sciences, Chinese Academy of Medical Sciences (Beijing, China). The microglia were seeded in a 6-well plate at a density of 1×10^6 cells each well. Briefly, the microglia were transfected with WT, WT + LPS, shMsrA + nonactive Tat-MsrA + LPS and shMsrA + Tat-MsrA + LPS. Among the latter three treatments, 0.01 ug/mL LPS was supplemented to the culture medium. After 18 h of pre-culture, the microglia were treated with 1 ug/mL LPS for 6 h, after which the cells were preserved for further experiments.

Statistical Analysis

The data collected from experiments were analyzed using the SPSS 21.0 statistical software (IBM Corp. Armonk, NY, USA). The measurement data were expressed as mean ± standard deviation. The unpaired *t*-test was adopted to compare data with normal distribution and homogeneous variance between two groups. The comparisons between multiple groups were analyzed by one-way analysis of variance (ANOVA), followed by Tukey's post hoc test. A value of $p < 0.05$ indicated that the difference was statistically significant.

Results

MsrA Exhibits Poor Expression in Cuprizone-Induced Mice

In order to analyze the expressions of MsrA, RT-qPCR (double internal reference genes GAPDH and β-actin) and Western blot analysis were performed in WT mice fed cuprizone and WT mice fed normal food over 4 weeks (Figure 1A and B). The result demonstrated a poor expression of MsrA in cuprizone-induced mice.

Aggravated Demyelination and Impaired Motor Coordination in Cuprizone-Induced MsrA $^{-/-}$ Mice

In order to ascertain the establishment of mouse model with demyelination, a series of experiments were performed. Western blot analysis was conducted to determine the expression of MsrA protein in the 20 normal WT mice and 20 MsrA-knockout mice (Figure 2A). The results showed that the MsrA expression was significantly reduced after silencing MsrA ($p < 0.05$). After instillation of cuprizone, the brain tissue sections of the mice were taken for model identification, and the degree of demyelination in cerebral corpus callosum as well as motor coordination ability in mice of each group was detected by performing Oil Red O staining and rotarod test (Figure 2B and C), respectively. No significant difference was observed in MsrA$^{-/-}$ mice compared to the relative controls ($p > 0.05$). Both of the WT or MsrA$^{-/-}$ mice had evident lipid-enriched myelin debris, demyelination, shorter dwell time in the rotation test, and the impaired motor coordination administrating cuprizone ($p < 0.05$), and the latter ones presented with even inferior results. Accumulating studies have confirmed that overexpression of Olig2 not only promotes the migration of oligodendrocyte precursor cells during embryonic development, the differentiation of oligodendrocytes and the early formation of myelin sheath, but also promotes myelin regeneration in adult demyelinated mice.[20–22] CNP, a fundamental marker of mature oligodendrocytes (the main component of myelin sheath), plays a vital supportive role in the oligodendrocyte skeleton. CNP may primitively appear in the early stage of

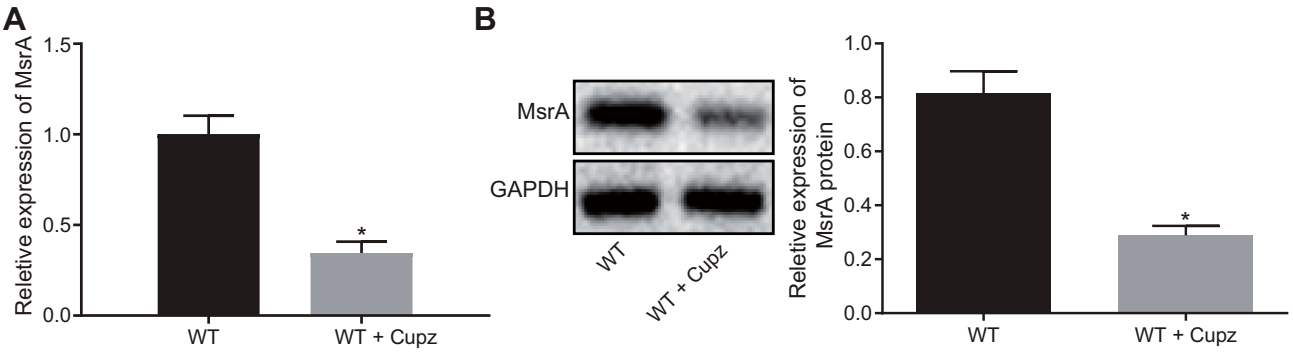

Figure 1 MsrA is down-regulated in cuprizone-induced mice. (**A**) detection of MsrA expression in cuprizone-induced mice by RT-qPCR, normalized to double internal reference genes GAPDH and β-actin. (**B**) detection of the MsrA protein expression in cuprizone-induced mice by Western blot analysis. *$p < 0.05$, compared to WT mice. The values are measurement data, expressed as mean ± standard deviation, and the unpaired *t*-test is used for data comparisons between two groups, N = 10.
Abbreviations: MsrA, Methionine sulfoxide reductase; WT, wild type; RT-qPCR, reverse transcription quantitative polymerase chain reaction.

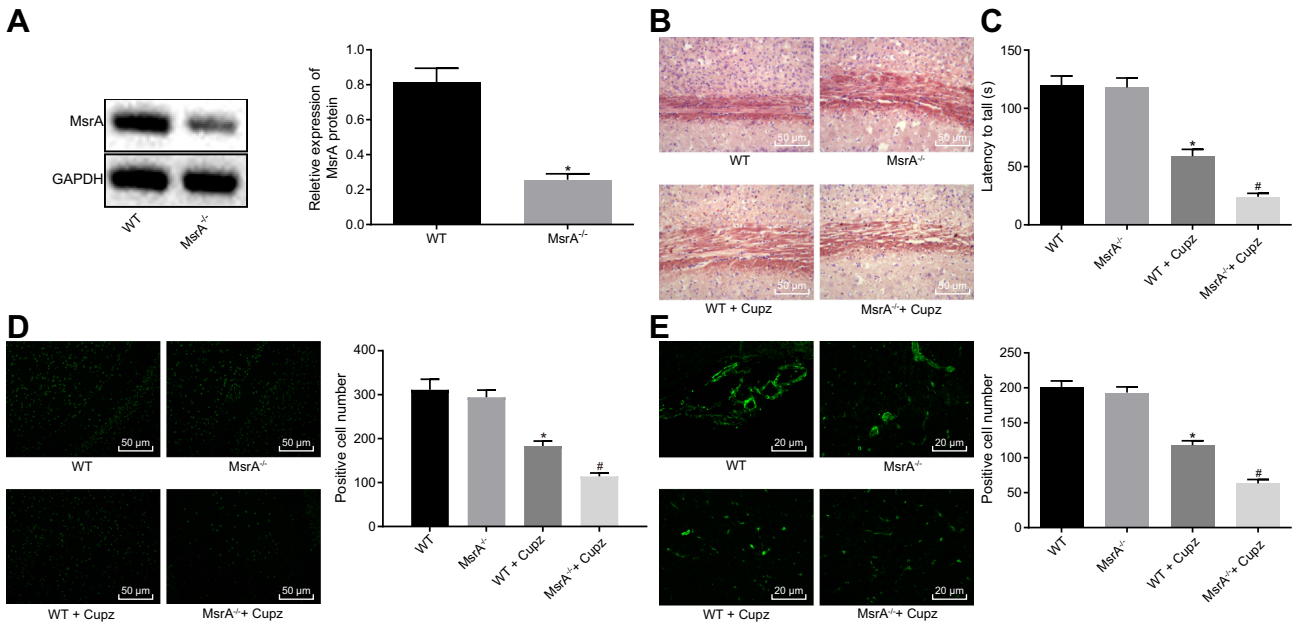

Figure 2 Cuprizone-induced MsrA$^{-/-}$ mice exhibit aggravated demyelination and impaired motor coordination. (**A**) detection of MsrA protein expression in WT mice and MsrA-knockout mice by Western blot analysis; (**B**) Oil Red O staining of demyelination in corpus callosum of mice (× 200, scale bar = 50 μm); (**C**) analysis of the motor coordination ability of mice by the rotarod test; (**D**) detection of Olig2-positive cells in corpus callosum by immunofluorescence assay (× 200, scale bar = 50 μm); (**E**) detection of CNP-positive cells in corpus callosum by immunofluorescence assay (× 400, scale bar = 25 μm). *$p < 0.05$, compared to WT mice; #$p < 0.05$, compared to WT mice treated with cuprizone. The values are measurement data, expressed as mean ± standard deviation, and the comparisons between multiple groups were analyzed by one-way ANOVA, followed by Tukey's post hoc test, N = 10.

Abbreviations: MsrA, Methionine sulfoxide reductase; WT, wild type; CNP, C-type natriuretic peptide; ANOVA, analysis of variance.

myelin sheath formation, accounting for about 4% of the whole central myelin sheath protein. In vitro studies have confirmed the critical function of CNP as a regulator of the growth of oligodendrocytes.[23,24] Thus, immunofluorescence assay was conducted to detect the number of Olig2-positive cells and CNP-positive cells in corpus callosum for further evaluation of demyelination. The results revealed that compared to the relative controls, no significant difference was evident in the MsrA$^{-/-}$mice ($p > 0.05$), while decreased number of Olig2-positive cells and number of CNP-positive cells were found in the WT + cuprizone group ($p < 0.05$). The number of Olig2-positive cells and number of CNP-positive cells decreased after treatment with MsrA$^{-/-}$ + cuprizone compared to treatment with WT + cuprizone ($p < 0.05$) (Figure 2D and E). The aforementioned results implied that cuprizone-induced MsrA$^{-/-}$ mice had aggravated demyelination and impaired motor coordination, thereby suggesting successful model establishment.

Exacerbated Inflammatory Reaction in Cuprizone-Induced MsrA$^{-/-}$ Mice

In order to investigate the inflammatory response of microglia in mice, immunofluorescence assay, Western blot analysis and ELISA were performed. After sectioning the brain tissues, the mouse microglia were isolated. Then immunofluorescence assay and Western blot analysis were conducted to detect the concentration of cerebral microglia markers including Iba1 (Figure 3A and B), and ELISA was conducted to detect the concentration of pro-inflammatory factors including TNF-α and IL-1β (Figure 3C). No significant difference was observed in the aforementioned factors between the WT and MsrA$^{-/-}$ mice ($p > 0.05$), while an increased Iba1 expression, as well as levels of TNF-α and IL-1β were detected in the WT + cuprizone group ($p < 0.05$). The Iba1 expression, as well as levels of TNF-α and IL-1β were increased significantly in the MsrA$^{-/-}$ + cuprizone group when compared with the WT + cuprizone group ($p < 0.05$). The aforementioned results elucidated that inflammation in microglia was exacerbated in cuprizone-induced MsrA$^{-/-}$ mice.

Microglia-Derived ROS Increases in Corpus Callosum of Cuprizone-Induced MsrA$^{-/-}$ Mice

In order to detect the expression of ROS in corpus callosum of cuprizone-induced MsrA$^{-/-}$ mice, immunofluorescence assay and Western blot analysis were conducted to determine the expression of 8-OHG in mouse microglia,

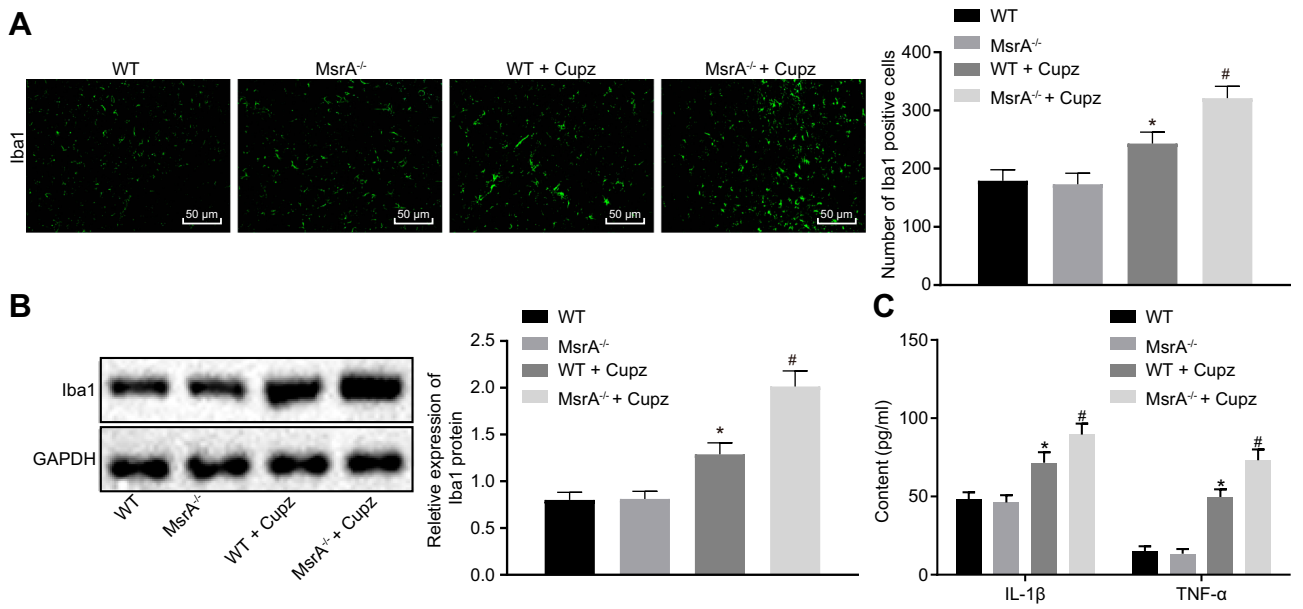

Figure 3 Inflammation of microglia is exacerbated in cuprizone-induced MsrA$^{-/-}$ mice. (**A**) detection of Iba1 expression means of in mouse microglia by immunofluorescence assay (× 200, scale bar = 50 μm); (**B**) detection of the Iba1 expression in mouse microglia by Western blot analysis; (**C**) detection of the expressions of various proinflammatory factors including TNF-α and IL-1β in mice by ELISA. *p < 0.05, compared to the WT mice. #p < 0.05, compared to WT mice treated with cuprizone. The values are measurement data, expressed as mean ± standard deviation, and the comparisons between multiple groups were analyzed by one-way ANOVA, followed by Tukey's post hoc test, N = 10.

Abbreviations: MsrA, Methionine sulfoxide reductase; WT, wild type; ELISA, enzyme-linked immunosorbent assay.

which suggested there was no substantial difference between WT mice and the MsrA$^{-/-}$mice (p > 0.05), while an elevated expression of 8-OHG was observed in the WT + cuprizone group (p < 0.05). In comparison with the WT + cuprizone group, the expression of 8-OHG in microglia had increased notably in the MsrA $^{-/-}$ + cuprizone group (p < 0.05; Figure 4A). Then the detection of intracellular ROS level and SOD activity was conducted, and the results showed that compared to the WT mice, there was no significant difference in MsrA-knockout mice (p > 0.05), while the level of ROS was elevated and SOD activity in mouse microglia was decreased in the WT + cuprizone group (p < 0.05). In addition, the level of ROS increased and the activity of SOD in mouse microglia decreased in the MsrA$^{-/-}$ + cuprizone group in comparison to the WT + cuprizone group (p < 0.05; Figure 4B and C). The aforementioned results suggested that the microglia-derived ROS was increased in corpus callosum in cuprizone-induced MsrA$^{-/-}$ mice.

NOX2-MAPKs/NF-κB Signaling Pathway Is Activated in LPS-Induced Microglia Upon MsrA Silencing

In order to corroborate the efficiency of transfection, Western blot analysis was conducted to detect the transfection efficiency after culturing mouse microglia in vitro. The results clarified that the expression of MsrA significantly decreased compared to the controls after treatment with sh-MsrA (p < 0.05) (Figure 5A), thereby suggesting successful transfection. In the following examination, the microglia-associated signaling pathway marker proteins were examined and the results revealed that compared with the sh-NC group, no significant difference was evident in the sh-MsrA group (p > 0.05), the expression of NOX2, and the extent of ERK, p38, IκBα, p65 and JNK phosphorylation were increased (all p < 0.05), while the expressions of ERK, p38, p65 and JNK denoted no significant differences (all p > 0.05); however the expression of IκBα decreased (p < 0.05) in the sh-NC + LPS group. In comparison to the sh-NC + LPS group, the sh-MsrA + LPS group presented with an increased NOX2 expression along with the extent of ERK, p38, IκBα, and p65 phosphorylation, decreased IκBα expression as well as no significant change in the expressions of ERK, p38, p65 and JNK as well as the extent of JNK phosphorylation (Figure 5B). Next, ELISA demonstrated no notable differences in the levels of TNF-α and IL-1β between the sh-NC and sh-MsrA groups (p > 0.05). In comparison to the sh-NC group, the up-regulated levels of TNF-α and

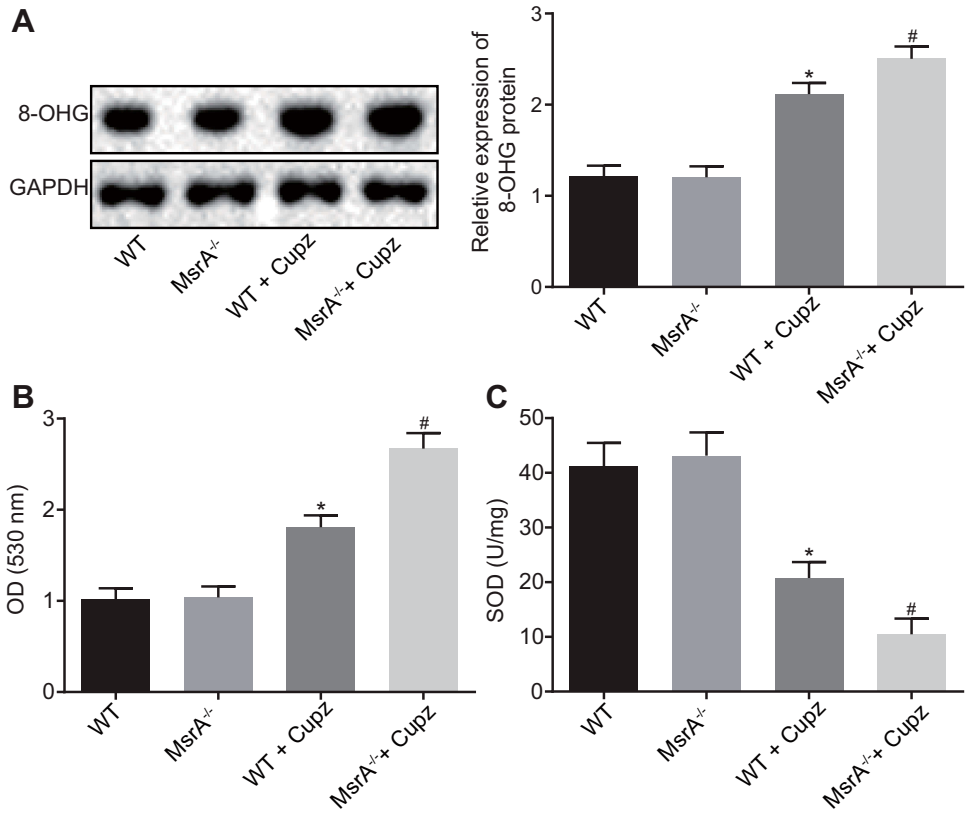

Figure 4 The expression of microglia-derived ROS is increased in corpus callosum of cuprizone-induced MsrA$^{-/-}$ mice. (**A**) detection of the expression of 8-OHG in mouse microglia by Western blot analysis; (**B**) detection of ROS; (**C**) detection of SOD activity. *p < 0.05, compared to WT mice. #p < 0.05, compared to WT mice treated with cuprizone. The values are measurement data, expressed as mean ± standard deviation, and one-way ANOVA is used for data comparisons among multiple groups, N = 10.
Abbreviations: ROS, reactive oxygen species; SOD, superoxide dismutase; 8-OHG, 8-hydroxyguanine; MsrA, Methionine sulfoxide reductase; WT, wild type.

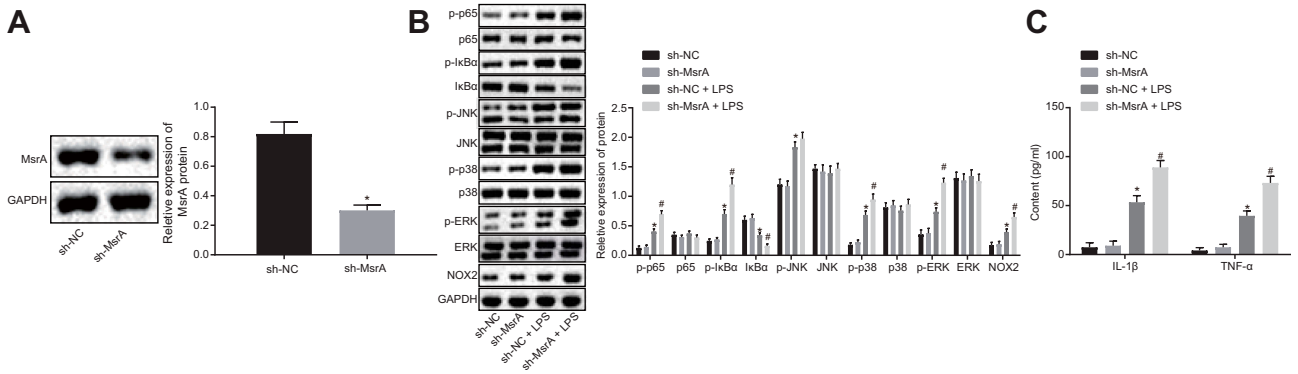

Figure 5 The NOX2-MAPKs/NF-κB signaling pathway is activated after LPS induction and MsrA silencing. (**A**) detection of transfection efficiency by Western blot analysis; (**B**) Western blot analysis of the NOX2-MAPKs/NF-κB signaling pathway-related proteins; (**C**) detection of the expression of inflammatory factors TNF-α and IL-1β by ELISA. *p < 0.05, compared to treatment with sh-NC; #p < 0.05, compared to treatment with sh-NC + LPS. The values are measurement data, expressed as mean ± standard deviation, and the comparisons between multiple groups were analyzed by one-way ANOVA, followed by Tukey's post hoc test, N = 10.
Abbreviations: JNK, c-Jun N-terminal kinase; ERK, extracellular-signal-regulated kinases; MsrA, Methionine sulfoxide reductase; LPS, lipopolysaccharide; NC, negative control; ELISA, enzyme-linked immunosorbent assay; ANOVA, analysis of variance.

IL-1β were observed in the sh-NC + LPS group (p < 0.05). Increased levels of TNF-α and IL-1β were also evident in the sh-MsrA + LPS group compared to the sh-NC + LPS group (p < 0.05; Figure 5C). The aforementioned results implied that after treatment with LPS induction and MsrA silencing, the NOX2-MAPKs /NF-κB signaling pathway was stimulated and the inflammation was intensified.

Tat-MsrA Fusion Protein Inhibits LPS-Induced Cellular Inflammatory Response by Negatively Regulating the NOX2-MAPKs/NF-κB Signaling Pathway

In order to substantiate the role of MsrA in demyelination, the microglia were treated with sh-NC, sh-NC + LPS, sh-MsrA + nonactive Tat-MsrA + LPS or sh-MsrA + Tat-MsrA + LPS, respectively. Firstly, detection of the activity of Tat-MsrA protein showed that the activity of Tat-MsrA protein increased following Tat-MsrA treatment compared to the nonactive Tat-MsrA treatment ($p < 0.05$; Figure 6A). Western blot analysis concluded (Figure 6B) that compared to matched control, the expression of NOX2 and the extent of ERK, p38, IκBα, p65 and JNK phosphorylation were increased (all $p < 0.05$), while the IκBα expression was decreased, the expressions of ERK, p38, p65, and JNK demonstrated no significant differences (all $p > 0.05$) after treatment of sh-NC + LPS ($p < 0.05$). However, the expression of NOX2 and the extent of ERK, p38, IκBα, and p65 phosphorylation were decreased (all $p < 0.05$), while IκBα expression was increased, the expressions of ERK, p38, p65 and JNK as well as the extent of JNK phosphorylation exhibited no significant differences (all $p > 0.05$) in the sh-MsrA + Tat-MsrA + LPS group compared to the sh-MsrA + nonactive Tat-MsrA + LPS group. The results of detection of intracellular ROS level and SOD activity suggested that compared with the relative controls, the level of intracellular ROS increased and SOD activity decreased after treatment with sh-NC + LPS (both $p < 0.05$). In comparison to the matched control, the level of intracellular ROS decreased while SOD activity increased in cells treated with sh-MsrA + Tat-MsrA + LPS (both $p < 0.05$; Figure 6C and D). Moreover, Western blot analysis demonstrated that in contrast to the sh-NC group, the expression of Iba1 increased

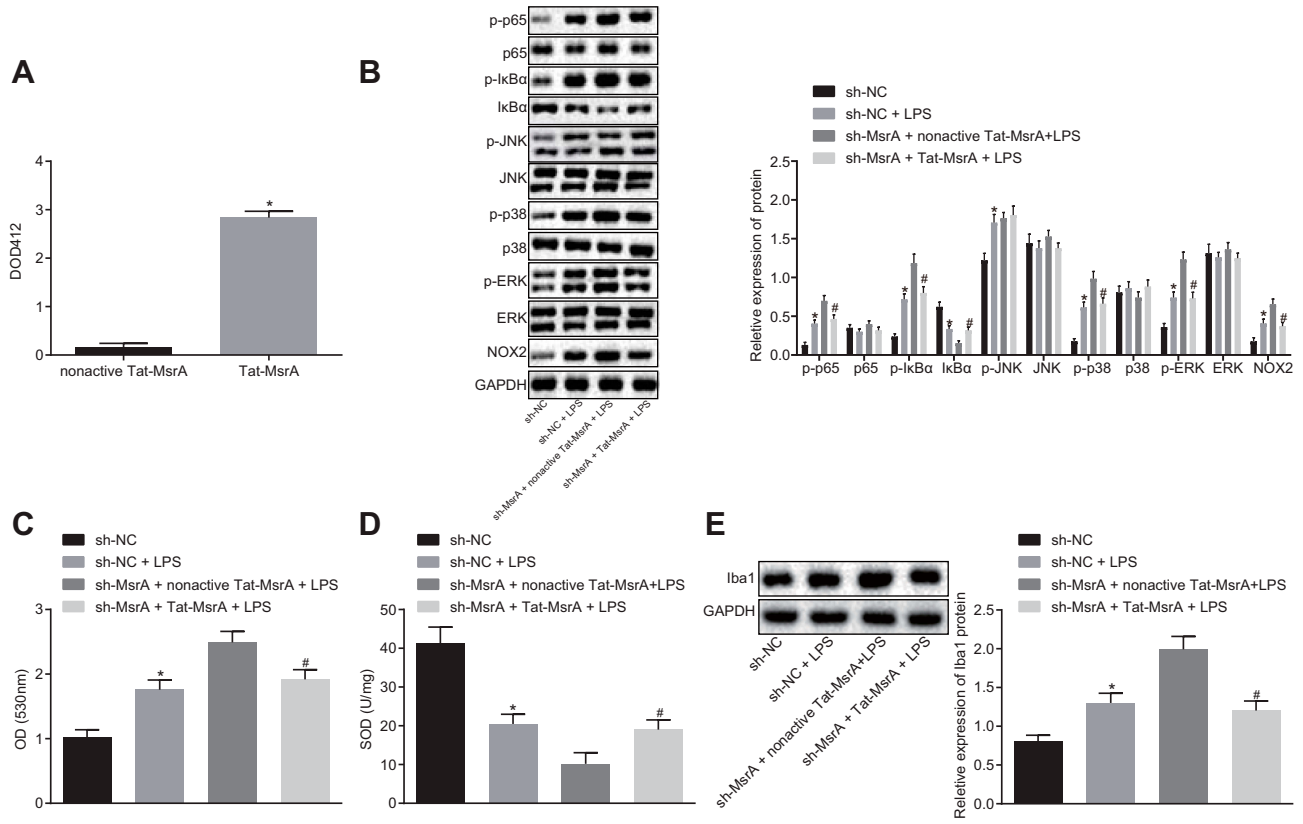

Figure 6 Tat-MsrA fusion protein suppresses LPS-induced cellular inflammatory response by inactivating the NOX2-MAPKs/NF-κB signaling pathway. (**A**) detection of the activity of Tat-MsrA fusion protein; (**B**) Western blot analysis of NOX2-MAPKs/NF-κB signaling pathway-related proteins in cells; (**C**) detection of intracellular ROS in cells; (**D**) detection of SOD activity; (**E**) Western blot analysis of Iba1 protein in cells. In panel (**A**), *$p < 0.05$, compared to treatment with nonactive Tat-MsrA. In panel (**B**–**E**), *$p < 0.05$, compared to treatment with sh-NC. #$p < 0.05$, compared to treatment with sh-MsrA + nonactive Tat-MsrA + LPS. The values are measurement data, expressed as mean ± standard deviation, and the comparisons between multiple groups were analyzed by one-way ANOVA, followed by Tukey's post hoc test, and the experiment was repeated three times.

Abbreviations: JNK, c-Jun N-terminal kinase; ERK, extracellular-signal-regulated kinases; MsrA, Methionine sulfoxide reductase; LPS, lipopolysaccharide; NC, negative control; ANOVA, analysis of variance.

in the sh-NC + LPS group ($p < 0.05$); while the expression of Iba1 decreased in the sh-MsrA + Tat-MsrA + LPS group compared to the sh-MsrA + nonactive Tat-MsrA + LPS group ($p < 0.05$; Figure 6E). The aforementioned results suggested that Tat-MsrA fusion protein suppressed LPS-induced cellular inflammatory response by negatively regulating the NOX2-MAPKs/NF-κB signaling pathway, thus preventing demyelination.

Discussion

Demyelination, a hallmark of MS, is a definite and functionally debilitating deficit, and it is a characteristic of several inflammatory diseases.[25] These diseases pose a heavy health burden for families with the highest prevalence in developed countries.[2] Previous studies suggest that in the central nervous system, multiple enzymes including NOX2 enzyme, and peripheral cholinergic enzymes are indicated in the treatment of demyelinating diseases.[26,27] However, the specific role of MsrA in demyelination remains largely unknown. The aim of our study was to offer a new perspective on the function of MsrA in demyelination and to obtain a deeper insight into the complexity of demyelination. Our study demonstrated that the MsrA fusion protein could potentially inhibit oxidative stress and inflammatory activation of microglia by negatively regulating the NOX2-MAPKs/NF-κB signaling pathway, thus preventing demyelination.

Initially, we found that MsrA exhibited a low expression in mouse demyelination models, which exacerbated the degree of demyelination. Partially in consistency with our findings, an existing study suggested that MsrA exhibited a poor expression in the brain tissues of patients with Alzheimer's disease, which is related to neuron degeneration and loss and further inhibits the resistance of neurons to oxidative damage.[28] Besides, a prior report have documented a reduced MsrA expression in the dopaminergic cells in Parkinson's disease.[29] Moreover, MsrA has been documented to be poorly expressed in several neurodegenerative diseases and loss of MsrA activity facilities oxidative stress, manifested by the accumulation of faulty proteins, deposition of aggregated proteins, and premature brain cell deaths.[30] These findings suggested the potential of a low level of MsrA in nervous system diseases and its deficiency to serve as a predictor for the risk of an adverse outcome in patients with the corresponding diseases.

Another key finding in our study was that MsrA silencing resulted in increased inflammatory activation in microglia and stimulated oxidative stress, illustrated by up-regulated Iba1, TNF-α and IL-1β levels as well as up-regulated ROS level and down-regulated SOD activity. Hyperactivation of microglia is recognized as a key manifestation of brain inflammation with vital function in mediating neuroinflammatory disorders.[31] MsrA, belonging to the methionine sulfoxide reductase family, can extensively decrease methionine sulfoxide concentration in proteins to further decrease oxidative stress.[32] Overexpression of MsrA protects the retinal pigment epithelial cells from oxidative stress and silencing or knockdown of MsrA reduces cell survival in degenerative diseases.[9] Silencing of MsrA can evidently exacerbate activation of microglia induced by LPS and increase the expression of relevant inflammatory markers.[15] It has been documented an association between Iba1 and inflammatory response and the interact of Iba1 with proteins fundamental for activation of the inflammatory response.[33] Both IL-1 and TNF are proinflammatory cytokines, the overexpression of which can lead to inflammation, fever, tissue destruction, and in severe circumstances even shock and death.[34] ROS are byproducts of aerobic metabolism, which induces mutilation to lipids, proteins and DNA, and oxidative stress refers to high intracellular expression of ROS.[35,36] Adenovirus-mediated upregulation of MsrA can significantly regress hypoxia-induced elevation in ROS levels and foster cell survival, thereby exhibiting the protective properties of MsrA against hypoxia/reoxygenation-induced cell injury and suggesting its therapeutic potential in ischemic heart and brain diseases.[37] The function of SOD has been identified in many inflammatory diseases, neurodegenerative diseases as well as ischemia and reperfusion diseases.[38] An existing study suggested that the overexpression of SOD-1 alleviated oxidative stress thereby solidifying the vitality of SOD-1 in oxidative stress protection.[39] These results demonstrate the protective properties of MsrA against microglia activation.

Another subsequent finding denoted the significance of activation of the NOX2-MAPKs/NF-κB signaling pathway in LPS-stimulated microglia upon MsrA silencing treatment. Evidence has indicated that the genetic and pharmacological inhibition of p38α, a p38 mitogen-activated protein kinases (MAPKs) isoform is associated with elevated NADPH oxidase (NOX2) activity.[40] Moreover, an existing study suggested that NADPH oxidases (NOXs), in sizeable fragment, mediated the production of ROS which was stimulated by LPS and NOX2 is a major NOX isoform observed in the macrophage cell membrane.[41] The aforementioned literature solidifies the

implication of NOX2 as an essential regulator of neurons. Evidence from another study suggested the activation of the MAPK/NF-κB signaling pathway in rat brain tissues after severe traumatic brain injury through upregulation of proteins pertinent to the MAPK signaling pathway and NF-κB nuclear translocation.[42] A further mechanistic study displayed that compound R6 treatment reduced the degree of LPS-induced MAPK-related protein (ERK, JNK and p38) phosphorylation and extensively reduced the degradation of IκB-α in BV2 microglial cells.[43] An existing study reported that upregulated MsrA could suppress ROS-augmented NF-κB signaling pathway activation in endothelial cells.[44] Furthermore, MsrA has been reported to negatively regulate microglia-mediated neuroinflammation through inhibition of the ROS/MAPKs/NF-κB signaling pathway in a catalytic antioxidant manner.[15] Therefore, we elucidated a potential downstream mechanism of the NOX2-MAPK/NF-kB signaling pathway in the progression of demyelination.

In conclusion, our study suggests that the Tat-MsrA fusion protein could potentially reduce oxidative stress and inflammatory activation of microglia to inhibit demyelination by suppressing the NOX2-MAPKs/NF-κB signaling pathway. Our data support that MsrA is a potential candidate marker and therapeutic target for demyelination in the central nervous system. However, due to the limitations of experimental funding and time, the downstream mechanism of the NOX2-MAPKs/NF-κB signaling pathway in the demyelination mouse models has not been studied in the present study, which proposes an avenue for future studies with comprehensive experiments.

Acknowledgment

We acknowledge and appreciate our colleagues for their valuable efforts and comments on this paper.

Author Contributions

Hua Fan, Damiao Li and Xinlei Guan designed the study. Yanhui Yang, Junqiang Yan and Jian Shi collected the data, carried out data analyses and produced the initial draft of the manuscript. Ranran Ma and Qing Shu contributed to drafting the manuscript. All authors contributed towards data analysis, drafting and critically revising the paper, gave final approval of the version to be published, and agreed to be accountable for all aspects of the work.

Funding

This study was supported by the National Natural Science Foundation of China (Grant/Award Number: U1504808, 81801201 and 81803503) and the Fundamental Research Funds for the Central Universities (Grant/Award Number: XZY012019121).

Disclosure

The authors report no conflicts of interest in this work.

References

1. Love S. Demyelinating diseases. *J Clin Pathol*. 2006;59(11):1151–1159. doi:10.1136/jcp.2005.031195
2. Popescu BF, Lucchinetti CF. Pathology of demyelinating diseases. *Annu Rev Pathol*. 2012;7:185–217. doi:10.1146/annurev-pathol-011811-132443
3. Weinshenker BG, Bass B, Rice GP, et al. The natural history of multiple sclerosis: a geographically based study. I. Clinical course and disability. *Brain*. 1989;112(Pt 1):133–146. doi:10.1093/brain/112.1.133
4. Wang D, Dong X, Wang C. Honokiol ameliorates amyloidosis and neuroinflammation and improves cognitive impairment in alzheimer's disease transgenic mice. *J Pharmacol Exp Ther*. 2018;366(3):470–478. doi:10.1124/jpet.118.248674
5. Yang JY, Xue X, Tian H, et al. Role of microglia in ethanol-induced neurodegenerative disease: pathological and behavioral dysfunction at different developmental stages. *Pharmacol Ther*. 2014;144(3):321–337. doi:10.1016/j.pharmthera.2014.07.002
6. Zhang HR, Peng JH, Cheng XB, et al. Paeoniflorin attenuates amyloidogenesis and the inflammatory responses in a transgenic mouse model of alzheimer's disease. *Neurochem Res*. 2015;40(8):1583–1592. doi:10.1007/s11064-015-1632-z
7. Mc Guire C, Beyaert R, van Loo G. Death receptor signalling in central nervous system inflammation and demyelination. *Trends Neurosci*. 2011;34(12):619–628. doi:10.1016/j.tins.2011.09.002
8. Raasch J, Zeller N, van Loo G, et al. IkappaB kinase 2 determines oligodendrocyte loss by non-cell-autonomous activation of NF-kappaB in the central nervous system. *Brain*. 2011;134(Pt 4):1184–1198. doi:10.1093/brain/awq359
9. Sreekumar PG, Hinton DR, Kannan R. Methionine sulfoxide reductase a: structure, function and role in ocular pathology. *World J Biol Chem*. 2011;2(8):184–192. doi:10.4331/wjbc.v2.i8.184
10. Wu Y, Xie G, Xu Y, et al. PEP-1-MsrA ameliorates inflammation and reduces atherosclerosis in apolipoprotein E deficient mice. *J Transl Med*. 2015;13:316. doi:10.1186/s12967-015-0677-8
11. Sorce S, Krause KH, Jaquet V. Targeting NOX enzymes in the central nervous system: therapeutic opportunities. *Cell Mol Life Sci*. 2012;69(14):2387–2407. doi:10.1007/s00018-012-1014-5
12. Fan B, Wang BF, Che L, et al. Blockage of NOX2/MAPK/NF-kappaB pathway protects photoreceptors against glucose deprivation-induced cell death. *Oxid Med Cell Longev*. 2017;2017:5093473. doi:10.1155/2017/5093473
13. Leung EL, Fan XX, Wong MP, et al. Targeting tyrosine kinase inhibitor-resistant non-small cell lung cancer by inducing epidermal growth factor receptor degradation via methionine 790 oxidation. *Antioxid Redox Signal*. 2016;24(5):263–279. doi:10.1089/ars.2015.6420
14. Yang CM, Hsieh HL, Yu PH, Lin CC, Liu SW. IL-1beta induces MMP-9-dependent brain astrocytic migration via transactivation of PDGF receptor/NADPH oxidase 2-derived reactive oxygen species signals. *Mol Neurobiol*. 2015;52(1):303–317. doi:10.1007/s12035-014-8838-y

15. Fan H, Wu PF, Zhang L, et al. Methionine sulfoxide reductase A negatively controls microglia-mediated neuroinflammation via inhibiting ROS/MAPKs/NF-kappaB signaling pathways through a catalytic antioxidant function. *Antioxid Redox Signal*. 2015;22(10):832–847. doi:10.1089/ars.2014.6022
16. Yamazaki R, Baba H, Yamaguchi Y. Unconventional myosin ID is involved in remyelination after cuprizone-induced demyelination. *Neurochem Res*. 2018;43(1):195–204. doi:10.1007/s11064-017-2413-7
17. Fan H, Zhao JG, Yan JQ, et al. Effect of notch1 gene on remyelination in multiple sclerosis in mouse models of acute demyelination. *J Cell Biochem*. 2018;119(11):9284–9294. doi:10.1002/jcb.27197
18. McIntosh A, Mela V, Harty C, et al. Iron accumulation in microglia triggers a cascade of events that leads to altered metabolism and compromised function in app/ps1 mice. *Brain Pathol*. 2019;29(5):606–621. doi:10.1111/bpa.v29.5
19. Liu J, Tian D, Murugan M, et al. Microglial Hv1 proton channel promotes cuprizone-induced demyelination through oxidative damage. *J Neurochem*. 2015;135(2):347–356. doi:10.1111/jnc.2015.135.issue-2
20. Mei F, Wang H, Liu S, et al. Stage-specific deletion of olig2 conveys opposing functions on differentiation and maturation of oligodendrocytes. *J Neurosci*. 2013;33(19):8454–8462. doi:10.1523/JNEUROSCI.2453-12.2013
21. Wegener A, Deboux C, Bachelin C, et al. Gain of olig2 function in oligodendrocyte progenitors promotes remyelination. *Brain*. 2015;138(Pt 1):120–135. doi:10.1093/brain/awu375
22. Copray S, Balasubramaniyan V, Levenga J, et al. Olig2 overexpression induces the in vitro differentiation of neural stem cells into mature oligodendrocytes. *Stem Cells*. 2006;24(4):1001–1010. doi:10.1634/stemcells.2005-0239
23. Gravel M, Robert F, Kottis V, et al. 2′,3′-cyclic nucleotide 3′-phosphodiesterase: a novel RNA-binding protein that inhibits protein synthesis. *J Neurosci Res*. 2009;87(5):1069–1079. doi:10.1002/jnr.v87:5
24. Lee J, Gravel M, Zhang R, et al. Process outgrowth in oligodendrocytes is mediated by cnp, a novel microtubule assembly myelin protein. *J Cell Biol*. 2005;170(4):661–673. doi:10.1083/jcb.200411047
25. Keirstead HS. Stem cells for the treatment of myelin loss. *Trends Neurosci*. 2005;28(12):677–683. doi:10.1016/j.tins.2005.09.008
26. Marrali G, Salamone P, Casale F, et al. NADPH oxidase 2 (NOX2) enzyme activation in patients with chronic inflammatory demyelinating polyneuropathy. *Eur J Neurol*. 2016;23(5):958–963. doi:10.1111/ene.2016.23.issue-5
27. Carvalho FB, Gutierres JM, Beckmann D, et al. Quercetin treatment regulates the Na(+), K(+)-ATPase activity, peripheral cholinergic enzymes, and oxidative stress in a rat model of demyelination. *Nutr Res*. 2018;55:45–56. doi:10.1016/j.nutres.2018.04.004
28. Gabbita SP, Aksenov MY, Lovell MA, Markesbery WR. Decrease in peptide methionine sulfoxide reductase in Alzheimer's disease brain. *J Neurochem*. 1999;73(4):1660–1666. doi:10.1046/j.1471-4159.1999.0731660.x
29. Liu F, Hindupur J, Nguyen JL, et al. Methionine sulfoxide reductase a protects dopaminergic cells from parkinson's disease-related insults. *Free Radic Biol Med*. 2008;45(3):242–255. doi:10.1016/j.freeradbiomed.2008.03.022
30. Pal R, Oien DB, Ersen FY, et al. Elevated levels of brain-pathologies associated with neurodegenerative diseases in the methionine sulfoxide reductase a knockout mouse. *Exp Brain Res*. 2007;180(4):765–774. doi:10.1007/s00221-007-0903-6
31. Bhatia HS, Baron J, Hagl S, et al. Rice bran derivatives alleviate microglia activation: possible involvement of MAPK pathway. *J Neuroinflammation*. 2016;13(1):148. doi:10.1186/s12974-016-0615-6
32. Lee JW, Gordiyenko NV, Marchetti M, et al. Gene structure, localization and role in oxidative stress of methionine sulfoxide reductase A (MSRA) in the monkey retina. *Exp Eye Res*. 2006;82(5):816–827. doi:10.1016/j.exer.2005.10.003
33. Maurya SK, Mishra R. Co-localization and interaction of Pax5 with Iba1 in brain of mice. *Cell Mol Neurobiol*. 2018;38(4):919–927. doi:10.1007/s10571-017-0566-1
34. Cerami A. Inflammatory cytokines. *Clin Immunol Immunopathol*. 1992;62(1 Pt 2):S3–S10. doi:10.1016/0090-1229(92)90035-M
35. Schieber M, Chandel NS. ROS function in redox signaling and oxidative stress. *Curr Biol*. 2014;24(10):R453–R462. doi:10.1016/j.cub.2014.03.034
36. Wang HW, Zhang Y, Tan PP, et al. Mitochondrial respiratory chain dysfunction mediated by ros is a primary point of fluoride-induced damage in hepa1-6 cells. *Environ Pollut*. 2019;255(Pt 3):113359. doi:10.1016/j.envpol.2019.113359
37. Yermolaieva O, Xu R, Schinstock C, et al. Methionine sulfoxide reductase a protects neuronal cells against brief hypoxia/reoxygenation. *Proc Natl Acad Sci U S A*. 2004;101(5):1159–1164. doi:10.1073/pnas.0308215100
38. McCord JM, Edeas MA. SOD, oxidative stress and human pathologies: a brief history and a future vision. *Biomed Pharmacother*. 2005;59(4):139–142. doi:10.1016/j.biopha.2005.03.005
39. Zheng Y, Liu Y, Ge J, et al. Resveratrol protects human lens epithelial cells against H2O2-induced oxidative stress by increasing catalase, SOD-1, and HO-1 expression. *Mol Vis*. 2010;16:1467–1474.
40. Liu L, Rezvani HR, Back JH, et al. Inhibition of p38 MAPK signaling augments skin tumorigenesis via NOX2 driven ROS generation. *PLoS One*. 2014;9(5):e97245. doi:10.1371/journal.pone.0097245
41. Meng T, Yu J, Lei Z, et al. Propofol reduces lipopolysaccharide-induced, NADPH oxidase (NOX 2) mediated TNF- alpha and IL-6 production in macrophages. *Clin Dev Immunol*. 2013;2013:325481. doi:10.1155/2013/325481
42. Chu W, Li M, Li F, et al. Immediate splenectomy down-regulates the MAPK-NF-kappaB signaling pathway in rat brain after severe traumatic brain injury. *J Trauma Acute Care Surg*. 2013;74(6):1446–1453. doi:10.1097/TA.0b013e31829246ad
43. Sun HN, Shen GN, Jin YZ, et al. 2-cyclohexylamino-5,8-dimethoxy-1,4-naphthoquinone inhibits lps-induced bv2 microglial activation through MAPK/NF-kB signaling pathways. *Heliyon*. 2016;2(7):e00132. doi:10.1016/j.heliyon.2016.e00132
44. Gu SX, Blokhin IO, Wilson KM, et al. Protein methionine oxidation augments reperfusion injury in acute ischemic stroke. *JCI Insight*. 2016;1(7). doi:10.1172/jci.insight.86460